Development of Accommodation Models for Soldiers in Vehicles: Driver

Yaser Zerehsaz
Sheila M. Ebert
Matthew P. Reed

Biosciences Group
University of Michigan Transportation Research Institute

September 2014

Development of Accommodation Models for Soldiers in Vehicles

Final Report

UMTRI-2014-26

by

Yaser Zerehsaz
Sheila M. Ebert
Matthew P. Reed

University of Michigan Transportation Research Institute

September 2014

REPORT DOCUMENTATION PAGE

Form Approved
OMB No. 0704-0188

1. REPORT DATE *(DD-MM-YYYY)*	**2. REPORT TYPE**	**3. DATES COVERED** *(From - To)*
September 27, 2014	Final Report	September 2013- September 2014

4. TITLE AND SUBTITLE

Development of Accommodation Models for Soldiers in Vehicles

5a. CONTRACT NUMBER
W56HZV-04-2-0001 P00038

5b. GRANT NUMBER

5c. PROGRAM ELEMENT NUMBER

6. AUTHOR(S)

Zerehsaz, Y., Ebert, S.M., and Reed, M. P.

5d. PROJECT NUMBER

5e. TASK NUMBER

5f. WORK UNIT NUMBER

7. PERFORMING ORGANIZATION NAME(S) AND ADDRESS(ES)

University of Michigan
Transportation Research Institute

8. PERFORMING ORGANIZATION REPORT

UMTRI-2014-26

9. SPONSORING / MONITORING AGENCY NAME(S) AND ADDRESS(ES)

US Army Tank Automotive Research,
Development, and Engineering Center

Warren, MI 48397-5000

10. SPONSOR/MONITOR'S ACRONYM(S)

11. SPONSOR/MONITOR'S REPORT NUMBER(S)
Issued Upon Submission

12. DISTRIBUTION / AVAILABILITY STATEMENT

13. SUPPLEMENTARY NOTES

14. ABSTRACT

Data from a previous study of soldier posture and position were analyzed to develop statistical models to define accommodation in driver and squad seating positions in military vehicles. Using methods previously developed for automotive applications, new models were created for seating accommodation, eye location, head (helmet) clearance, knee clearance, and torso clearance. The resulting models are applicable to driver positions with a fixed heel point and a range of steering wheel locations typical of tactical vehicles. The models were developed based on driver posture data but could be used for other front seat environments (e.g., commander position) with certain assumptions. All of the models include the effects of body armor and body borne gear.

15. SUBJECT TERMS
Anthropometry, Posture, Vehicle Occupants, Accommodation

16. SECURITY CLASSIFICATION OF:			**17. LIMITATION OF ABSTRACT**	**18. NUMBER OF PAGES**	**19a. NAME OF RESPONSIBLE PERSON**
UNCLASSIFIED: Dist. A. Approved for public release.					M.P. Reed
a. REPORT	**b. ABSTRACT**	**c. THIS PAGE**			**19b. TELEPHONE NUMBER** *(include area code)*
TBD	TBD	TBD		51	(734)936-1111

Standard Form 298 (Rev. 8-98)
Prescribed by ANSI Std. Z39.18

ACKNOWLEDGMENTS

This research was supported by the Automotive Research Center (ARC) at the University of Michigan under agreement W56H2V-14-2-0001 with the US Army Tank Automotive Research, Development, and Engineering Center (TARDEC) in Warren, MI. We thank Gale Zielinski and Frank Huston of TARDEC for their assistance and support for the project, including careful review of the models and documentation presented in this report. We also thank Prof. Judy Jin from the Department of Industrial and Operations Engineering for her thoughtful contributions.

CONTENTS

ABSTRACT

Data from a previous study of soldier posture and position were analyzed to develop statistical models to define accommodation in driver and squad seating positions in military vehicles. Using methods previously developed for automotive applications, new models were created for seating accommodation, eye location, head (helmet) contour, knee contour, and torso contour. The resulting models are applicable to driver positions with a fixed heel point and a range of steering wheel locations typical of tactical vehicles. The models were developed based on driver posture data but could be used for other front seat environments (e.g., commander position) with certain assumptions. All of the models include the effects of body armor and body borne gear.

INTRODUCTION

The design of military vehicles in the United States is guided in part by Military Standard (MILSTD) 1472G, Human Engineering, a design standard that encompasses a broad array of normative data for human needs and performance. A small section of this standard addresses the design of vehicle seats and the layout of the driver workstation. However, this guidance is out of date and incomplete in many respects. For example, the standard is not based on distributions of soldier body dimensions from modern studies, does not specify appropriate ranges of seat adjustment, and does not adequately take into account the effects of body armor on driver posture and position.

The automobile industry has long used more sophisticated tools for designing and assessing occupant accommodation. During the 1950s, template-based design approach that represented the human body (usually a midsize male) as a kinematic linkage began to be used (Dempster 1955, Geoffrey 1961). Because template-based approaches, including modern methods using three-dimensional Computer-aided design (CAD) manikins, cannot provide precise estimates of accommodation, Meldrum (1965) introduced the eyellipse, the first of what became known as population accommodation models. The eyellipse is a geometric representation of the distribution of drivers' eye locations based on a multinormal approximation. The critical insight in the development of the eyellipse was that it was necessary to combine the effects of vehicle layout and driver anthropometric variability into a single tool. The eyellipse was adopted as an industry standard in Society of Automotive Engineers (SAE) J941, and other related tools followed in the 1970s and 1980s (Hammond and Roe 1972): hand control reach (SAE J287), seating accommodation (SAE J1517), and head clearance (SAE J1052). SAE J941 was completely revised in 2002 using a new model developed at UMTRI (Manary et al. 1998). SAE J1517 was superseded in 2004 by a SAE J4004, which incorporates a new seating accommodation model developed at the University of Michigan Transportation Research Institute (UMTRI) (Flannagan et al. 1998).

Although the current generation of automotive accommodation models could be applied to military vehicle design, several problems are evident. The application range for these models is SAE Class A, which is limited to seat heights (SAE H30) of 405 mm or lower. Many military trucks have higher seat heights. Most importantly, the models do not take into account the effects of body armor or body borne gear on Soldier posture and position.

During the 1980s, analogous models were developed for SAE Class B vehicles, i.e., trucks and buses. The tools were all based on the same dataset (Sanders and Shaw 1985, Phillipart et al. 1985, Stanick et al. 1987) obtained in a laboratory study of truck drivers. The eyellipse and seating accommodation models were incorporated into SAE J941 and J1517, respectively, with important locating procedures embodied in SAE J1516. Additional models only for Class B were published in

separate recommended practices: driver shin/knee contour (SAE J1521) and belly contour (SAE J1522).

In the late 1990s, UMTRI and industry collaborators conducted a laboratory study and a test-track, in-vehicle study aimed at overcoming the limitations of the Sanders and Shaw study and the resulting design tools (Reed et al. 2000, Jahns et al. 2001). The testing configurations included height-adjustable seats and a wide range of steering wheel positions, spanning most of the practical Class-B range. The data were used to create posture-prediction models as well as a new eyellipse and seating accommodation model (Reed et al. 2005) and new knee, head, and belly clearance models (Reed et al. 2006). These UMTRI Class-B models have been widely used for vehicle design over the past 10 years.

However, both the SAE practices and the more recent UMTRI models have important limitations for military vehicle design. The SAE models do not include the effects of height adjustable seats, or seats with adjustable back angles. Unlike the new generation of automotive (Class-A) models, the SAE Class-B models are not parametric for population body dimensions, and hence can't be adjusted to target an Army population. Neither the SAE nor UMTRI Class-B models incorporate the effects of body armor or body borne gear.

The current study closely follows the recent UMTRI development of Class-B models, except that the data used are from the Seated Soldier Study (Reed et al. 2013), a large-scale laboratory study of Soldier posture and position as drivers and passengers (squad). The study was designed to focus on tactical vehicle (truck) designs with fixed driver heel points and H30 values spanning the upper end of the SAE Class-A range and the lower end of the SAE Class-B range. In this way, the data span the gap between UMTRI's previous automotive and commercial vehicle models. This report presents the methods and outputs for new driver eyellipse and seating accommodation models, as well as driver knee contour, torso contour with body armor and body borne gear, and head contours taking into account the helmet.

METHODS

Data Source and Applicable Ranges

The data used for the current analysis were gathered in the Seated Soldier Study (Reed and Ebert 2013). Posture and position data were recorded for male and female enlisted personnel at three Army posts as they sat in a driver mockup (Figure 1).

Figure 1. Driver and squad mockups.

The current study used data from 145 men and women tested in the driver mockup. Table 1 lists summary statistics for standard anthropometric variables for the combined male/female population. (For single-gender populations and distribution data for more anthropometric measures, see the Seated Soldier report.)

Table 1
Anthropometric Characteristics of the Driver Population (combined men and women)

Variable	Mean	SD	5th%ile	50th%ile	95th%ile
Stature (mm)	1726	74.2	1589	1734	1840
Body Weight (kg)	78.7	13.3	58.1	76.5	102.4
Erect Sitting Height (mm)	902	40.6	831	905	977
Sitting Height / Stature	0.523	0.0135	0.497	0.523	0.545
BMI (kg/m^2)	26.4	3.9	20.3	26.5	33.2

Figure 2 shows the garb levels used for measurements in the mockup. At the Advanced Combat Uniform (ACU) level, Soldiers wore their own advanced combat uniform consisting of a jacket, trousers, moisture wicking shirt and brown combat boots. All items were removed from the pockets, extra padding removed from the knees, and any cap or helmet removed. At the Personal Protective Equipment (PPE) level, Soldiers wore an Improved Outer Tactical Vest (IOTV) with Enhanced Small Arms Protective Insert (ESAPI) plates, Enhanced Side Ballistic Inserts (ESBI), and an Advanced Combat Helmet (ACH) over their ACU ensemble. Five sizes of IOTV were available at the study site. The Soldiers were given their self-reported sizes of helmet and IOTV with front, back and side plates. The investigator helped the Soldier don the PPE and checked the fit. The fit was considered acceptable if (1) the elastic waistband of the IOTV was snug with the Velcro closure fully overlapped and (2) the bottom of the IOTV was located below the navel and above the belt. The Soldiers wore the smallest size helmet in which the Soldier's head was in contact with the padding on the inside of the top of the helmet.

The third level of gear was referred to as encumbered (ENC), which consisted of ACU, PPE, a hydration pack, and a Tactical Assault Panel (TAP). Figure 2 shows a soldier in the three levels of gear, including both versions of ENC (rifleman and SAW gunner). The rifleman kit was used for all driver data collection.

ACU PPE ENC (Rifleman)

Figure 2. Three levels of military garb worn during measurement: ACU, PPE and ENC (left to right).

Table 2 shows the driver mockup conditions, which were presented in random order at the ACU level of garb. Condition 5 was repeated at the PPE and ENC (rifleman) levels. In each condition, the seat was initially adjusted to the mean expected position for male Soldiers based on previous research and the seat back

angle was set to 17 degrees. The Soldier entered the mockup and adjusted the seat fore-aft and vertically, along with adjusting the seat back angle, to obtain a comfortable driving position. The Soldier's posture and seat adjustments were recorded by digitizing body and seat landmarks using a FARO Arm coordinate digitizer. The seat position was expressed as the SAE J826 H-point location relative to the accelerator heel point (AHP). Seat back angle was expressed relative to the SAE J826 manikin torso angle with respect to vertical (SAE A40).

Table 2
Condition Matrix for Driver Mockup

	Accelerator Heel Point Relative to Steering Wheel		Accelerator Pedal Angle	Initial Seat H-point Relative to Steering Wheel	Seat Height
Package†	SAE L11, Fore-Aft (mm)	SAE H17, Vertical (mm)	Degrees from horizontal	Fore-Aft (mm)	SAE H30 (mm)
1	225	785	47	417	473
3	375	785	47	364	473
5*	337.5	735	40	390	423
7	300	685	33	417	373
9	450	685	33	364	373

*Repeated with PPE and ENC
† Conditions 2, 4, 6, and 8 were dropped after the first few sessions due to time constraints. The original condition numbers were retained for consistency with earlier documentation.

In general, the models presented in this report are valid over the range of conditions present in the underlying data. However, a small amount of extrapolation is reasonable given the linear trends observed in this work and experience in previous studies with driver and passenger postures. Table 3 lists the relevant ranges of individual parameters including maximum recommended extrapolation. Note that the reasonable ranges of some variables are dependent on the range of other variables (e.g., steering wheel height and steering wheel fore-aft location). In general, errors will be larger with greater extrapolation, but it's not feasible to calculate those errors, due to uncertainty about how occupants would respond in the extrapolated conditions. The driver data collection conditions included a 350-mm-diameter steering wheel at a fixed 45-degree angle. Based on previous studies showing minimal effects of steering wheel diameter and angle, the current models should be valid across a reasonable range of these variables, e.g., 200- to 450-mm-diameter and 15 to 55-degree steering wheels. The results are also likely applicable to yoke-type steering arrangements, using the midpoint between the hand grips as the reference point for location.

Table 3
Applicable Ranges, Driver Models (mm)

Variable	Lower Range, Extrapolated	Lower Range in Data	Upper Range in Data	Upper Range, Extrapolated
Seat Height (H30)*	350	373	473	500
Steering Wheel Height (H17)*	660	685	785	810
Steering Wheel Fore-aft Position (L11)*	200	225	450	475

* Reasonable values of H30 depend on H17.
** H17 and L11 should be considered together.

Data Analysis – General Modeling Approach

The data analysis and model development in this report are based on linear regression analysis and exploit some of the statistical characteristics of linear functions of variables that follow a normal distribution. In general, a dimension of interest, such as fore-aft seat position, is expressed as a linear function of potential predictors, such as steering wheel position and driver stature. The models have the form

$$y = c_0 + c_1 x_1 + c_2 x_2 + \ldots + e(0, s^2) \qquad [1]$$

where y is the dependent measure to be predicted, the c_i are constant coefficients obtained by fitting to the data, the x_i are the predictors (vehicle and driver body dimensions). The final "error" term $e(0, s^2)$ is a random, normally distributed variable with zero mean and variance s^2, where s is the root mean square error (RMSE) of the regression. In computational terms, the RMSE is the standard deviation of the data vector that is obtained by subtracting the regression prediction from each data observation. This residual variance is a crucial part of the modeling in this report.

Figure 3 shows a linear regression for fore-aft seat position, using (for purposes of illustration) stature as a single predictor. The residual variance, quantified by the mean square error, is modeled as normal distribution centered on the predicted value. Under the assumptions of linear regression, the residual variance is independent of the predictors. The analysis of the driver posture data shows that this assumption is well supported for these models. As an example of the interpretation of the constant-variance assumption, the standard deviation of fore-aft eye location for men who are 1700 mm tall is the same as the standard deviation of fore-aft eye location for men who are 1800 mm tall. Data from men and women are merged for all of the analyses in this report, because the statistical analysis in the Seated Soldier Study showed no important gender differences not accounted for by body size.

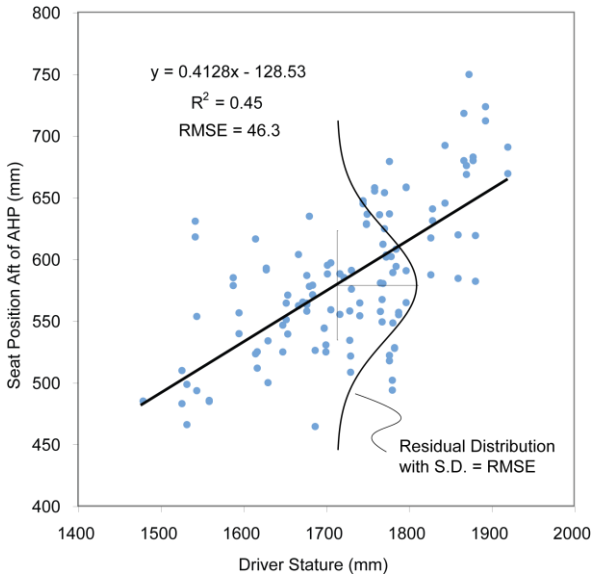

Figure 3. Plot of stature vs. fore-aft seat position to illustrate regression analysis principles.

The model development procedure in this report exploits an important feature of normal distributions, which is that the mean and standard deviation of a linear function of a normal distribution is also a normal distribution. Specifically, if

$$Y = c_0 + c_1 X \quad [2]$$

where c_0 and c_1 are constants and X is a normal distribution with mean X_{Mean} and standard deviation s_X, then Y is also a normal distribution, with mean

$$Y_{Mean} = c_0 + c_1 X_{Mean} \quad [3]$$

and variance (standard deviation squared) of

$$s_Y^2 = (c_1 s_X)^2 \quad [4]$$

The sum of two normal distributions is also a normal distribution, with variance equal to the sum of the variances. So, the residual variance from a regression can be included in estimating the distribution of the dependent measures. For example, consider

$$HPtX = c_0 + c_1 Stature + e(0, s^2) \quad [5]$$

where $HPtX$ is fore-aft seat position, c_0 and c_1 are constant coefficients from the regression analysis, and s is the root mean square error from the regression. If stature is modeled as a normally distributed random variable, this becomes the sum

of two normally distributed random variables. Hence, for this example, *HPtX* is modeled as a normal distribution with mean

$$HPtX_{\text{Mean}} = c_0 + c_1\, Stature_{\text{Mean}} \quad [6]$$

and variance

$$s_{\text{Stature}}^2 = (c_1\, s_{\text{Stature}})^2 \quad [7]$$

This formulation is particularly valuable for modeling driver posture because the relevant human descriptors, such as stature and body mass index, are approximately normally distributed within gender or can be transformed to be. If the predictors are correlated, then the calculation of the variance of the independent is slightly different. For the equation

$$Y = c_1\, X_1 + c_2\, X_2 \quad [8]$$

where X_1 and X_2 are normally distributed random variables with variances s_1^2 and s_2^2 and correlation $r_{1,2}$, the variance of Y is given by

$$s_Y^2 = (c_1\, s_1)^2 + (c_2\, s_2)^2 + 2\, r_{1,2}\, s_1\, s_2 \quad [9]$$

For a difference between two normal random variables

$$Y = c_1\, X_1 - c_2\, X_2 \quad [10]$$

the covariance ($r_{1,2}\, s_1\, s_2$) is subtracted:

$$s_Y^2 = (c_1\, s_1)^2 + (c_2\, s_2)^2 - 2\, r_{1,2}\, s_1\, s_2 \quad [11]$$

In general, the occupant population includes both men and women. Although single-gender distributions of many anthropometric variables can be accurately approximated as normal distributions, the male and female components must usually be modeled separately. The level of accommodation for each gender is computed and the respective fractions are combined using the population gender mix. For example, if the fraction of males in the population is m, the total fraction accommodated is

$$F_{\text{total}} = m\, (F_{\text{m}}) + (1\text{-}m)\, F_{\text{f}} \quad [12]$$

where F_m and F_f are the fractions of male and female occupants accommodated, respectively.

Eye locations can be effectively represented by a multivariate normal distribution. In sideview, a bivariate normal distribution is represented by a mean vector $\{X_{1,\,\mathrm{Mean}}, X_{2,\,\mathrm{Mean}}\}$ and a covariance matrix

$$V = \begin{bmatrix} s_{X_1}^2 & r_{1,2}s_1s_2 \\ r_{1,2}s_1s_2 & s_{X_2}^2 \end{bmatrix} \qquad [13]$$

The first eigenvector of the covariance matrix, which is equivalent to the first principal component of the data, is the direction along which the data have the greatest variance. These calculations are used to determine the appropriate orientation for the eyellipse.

Data Analysis – Seat Position

The goal of the seating accommodation modeling is to create a statistical model of the expected distribution of driver-selected seat positions given the vehicle configuration and the population description. The analysis methodology is described in detail in Reed (2005). Linear regression analyses were conducted to express the fore-aft and vertical seat position with respect to AHP as a function of steering wheel position and subject attributes. The regression results are tabulated in Reed and Ebert (2013) and are repeated in this report in the Results section.

The calculations identify the percentage of drivers whose preferred seat position (translated seat H-point location) will be accommodated by a particular seat track arrangement. For purposes of this analysis, the seat track is assumed to provide both vertical and fore-aft adjustment, so that the seat adjustment range can be represented by a rectangle in side view.

In practice, a designer will likely want to accommodate a target percentage of drivers on fore-aft and vertical position simultaneously. Suppose the target is 95% accommodation on both vertical and fore-aft seat positions. The total percentage disaccommodated is the sum of the fractions disaccommodated on the front, back, top, and bottom of the adjustment range, minus the double-counted individuals in the corners. Because fore-aft and vertical seat positions are uncorrelated in this dataset, the corner fractions are simply the product of the adjacent fractions. For example, if 2.5% of drivers are disaccommodated at the top of the travel and 2.5% at the front of the travel, the percentage of drivers who prefer a seat position both above and forward of the adjustment range is $(0.025)^2 = 0.0006225$. With symmetrical disaccommodation of p in each of the four directions, the total accommodation A is

$$A = 1 - 4\,p + 4\,p^2 \qquad [14]$$

Solving the quadratic equation for p gives

$$p = 0.5 - 0.5\,(A)^{1/2} \qquad [15]$$

So, to accommodate the central 95% of the population, the disaccommodation at the top, bottom, front, and back of a rectangular seat track must each be not more than approximately 1.3%.

Data Analysis – Eye Location

The eyellipse has a "cutoff" characteristic illustrated schematically in Figure 4. Under the reasonable assumption that the underlying eye location distribution is multinormal, all tangents to the eyellipse (either a line in 2D or a plane in 3D) divides the eye location distribution into constant fractions. For example, a tangent to the commonly used "95% eyellipse" divides the eye location distribution into 95%/5% fractions. This characteristic is exploited for vision analyses in which the goal is to ensure that a desired percentage of the driver population can see a particular internal or external target without head movement. Figure 4 shows an upvision analysis, demonstrating the maximum upvision angle that would accommodates 95% of the driver population.

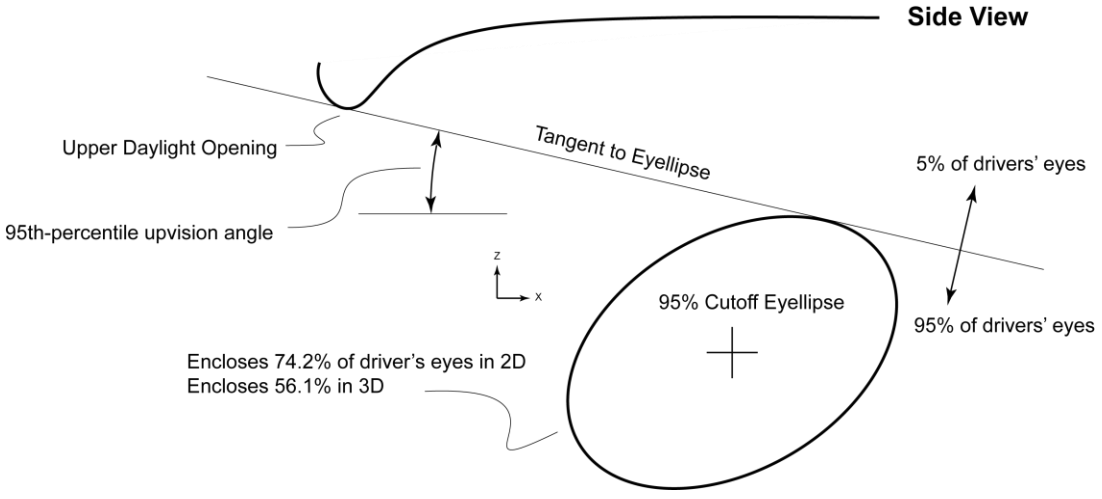

Figure 4. Illustration of side-view eyellipse with 95% cutoff characteristic.

The construction of the eyellipse is divided into two stages. First, the dimensions of the eyellipse are determined. Second, the eyellipse is located in the package with respect to the AHP. The eyellipse is used with the seating accommodation model presented in the previous section. In fact, the first step in the process of locating the

new eyellipse within the vehicle package is calculating the mean fore-aft and vertical seat position.

The eyellipse was developed using statistical procedures that are very similar to those that were used to develop the Class-B eyellipse. As with the seat-position model, the eyellipse is configurable for the body dimension distributions of the driver population and gender mix. The eyellipse models the distribution of driver eye locations as a three-dimensional normal distribution. Specifically, the data analysis suggests that the distribution of right or left eye locations for a single gender population in a vehicle with minimal censoring due to seat track limitations, headroom, knee room, and other clearance dimensions will be normal on each axis. Because the male and female eye location distributions overlap substantially, and because conducting analyses with separate male and female eyellipses would be cumbersome, a procedure has been developed to create a single eyellipse that approximates the cutoff behavior that would be obtained through weighted analyses using single-gender eyellipses.

Figure 5 shows the process schematically. An analysis of the eye location data showed that, due to shorter drivers sitting further forward, the eyellipse is inclined down at the front. Male and female centroids are computed along the inclined x' axis based on the mean statures and mean seat positions for both single-gender populations. Front and rear cutoffs are then computed for the combined male-female population, using the same methods applied to seat position calculations. The vertical (z') and lateral (y) dimensions are computed similarly using normal-distribution approximations.

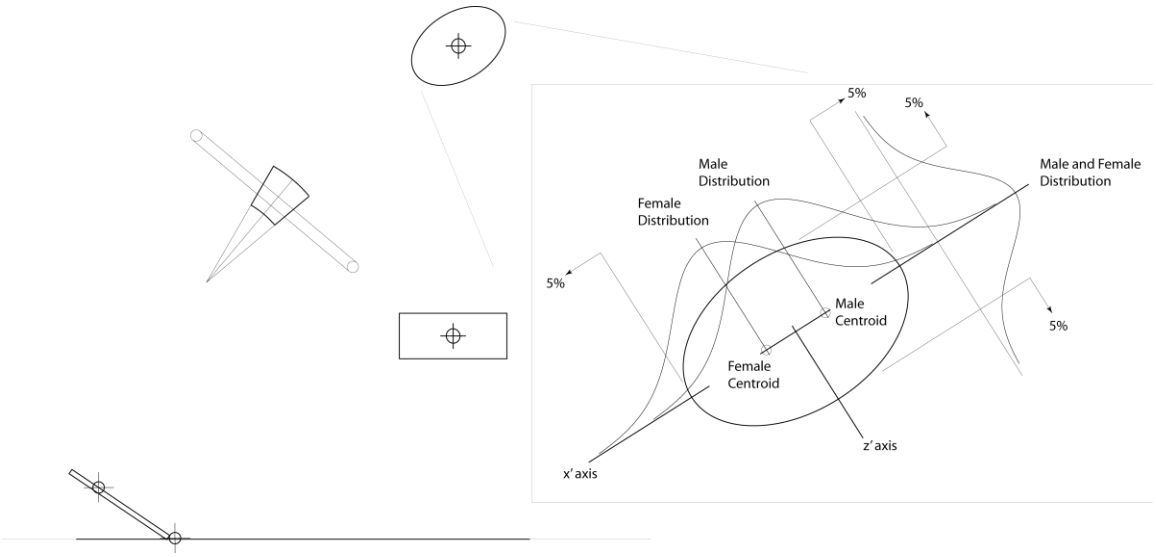

Figure 5. Schematic of eyellipse construction. A similar procedure is used for the Z' axis.

RESULTS

Seating Accommodation

Table 4 shows the linear regression equations from Reed and Ebert (2013) for predicting driver-selected fore-aft and vertical seat position. For demonstration purposes, we use the anthropometric distributions from the Army Anthropometric Survey (ANSUR) (Gordon et al. 1989) shown in Table 5. Fore-aft steering position is represented by the relative L11 value ($L11_{rel}$), which is computed as L11 - (888.75 - 0.75 H17). In the data, $L11_{rel}$ takes on values of -75, 0, and 75 mm, but the resulting models can be used with any $L11_{rel}$ value.

Table 4
Linear Regression Models for Predicting Fore-aft and Vertical Seat Positions (ACU)

Mean	intercept	L11rel*	H17	Stature	Ln(BMI)	Sitting Height (SH)/Stature (S)	R^2_{adj}	RMSE
μ_x	1014	0.487	-0.780	0.310	62.2	-923	0.75	30.3
μ_z	-252	-0.089	0.99	-0.037			0.80	20.8

* $L11_{rel}$ = L11 - (888.75 - 0.75 H17); $L11_{rel}$ takes on values of -75, 0, and 75 mm.

Table 5
Anthropometric Data from ANSUR Used for Example Calculations (Gordon et al. 1989)

Dimension (mm)	Men	Women
Stature (S)	1756 (66.8)	1629 (63.5)
Ratio of Erect Sitting Height to Stature (SH/S)	0.521 (0.0144)	0.523 (0.0146)
Log(BMI)†	3.23 (0.117)	3.14 (0.112)

* Means and standard deviations estimated to obtain an accurate fit at the 5th and 95th percentiles of the distributions when using a normal approximation. These are not necessarily the actual means and standard deviations of the data.
† Units are *natural log* (kg/m^2)

Garb effects are applied to the mean values calculated using the ACU equations in Table 4. The mean seat positions are shifted rearward by 20.8 and 64.7 mm for PPE and ENC conditions, respectively.

Using the equations from Table 4 and values from Table 5 we calculate:

$$\mu_{seatposition,male} = 1278.8 - 0.780\ H17 + 0.487\ L11_{rel} \quad [16]$$

$$\mu_{seatposition,female} = 1231.9 - 0.780\ H17 + 0.487\ L11_{rel} \quad [17]$$

$$\sigma_{seatpositionx,male} = \sqrt{(0.310\sigma_{Stature,male})^2 + (62.3\sigma_{\ln(BMI),male})^2 + (-923\sigma_{SH/S,male})^2 + (30.3)^2} = 39.7$$ [18]

$$\sigma_{seatpositionx,female} = \sqrt{(0.310\sigma_{Stature,female})^2 + (62.3\sigma_{\ln(BMI),female})^2 + (-923\sigma_{SH/S,female})^2 + (30.3)^2}$$ = 39.2 [19]

Because stature, ln (BMI) and Sitting Height (SH)/Stature (S) are minimally correlated in this dataset, the last two equations overlook the covariance among these variables in computing the standard deviation of seat position X.

Now, we are able to determine the fore-aft seat adjustment range that is needed to accommodate a desired percentage of the mixed-gender population. Taking *m* as the fraction of male in a population, the total disaccommodated fraction of the two-gender population lying forward of x_1 is

$$F_1 = m\left[\phi\left(\frac{x_1 - \mu_{seatpositionx,male}}{\sigma_{seatpositionx,male}}\right)\right] + (1-m)\left[\phi\left(\frac{x_1 - \mu_{seatpositionx,female}}{\sigma_{seatpositionx,female}}\right)\right] \quad [20]$$

where $\phi(z)$ is the cumulative standard normal distribution. Analogously, the fraction of the combined male and female population which lies rearward of x_2 can be given by

$$F_2 = m\left[1-\phi\left(\frac{x_2 - \mu_{seatpositionx,male}}{\sigma_{seatpositionx,male}}\right)\right] + (1-m)\left[1-\phi\left(\frac{x_2 - \mu_{seatpositionx,female}}{\sigma_{seatpositionx,female}}\right)\right] \quad [21]$$

Since there is no closed-form solution to x_1 and x_2, a solution is obtained by iteration of x_1 and x_2 to obtain the desired accommodation level. A similar procedure is followed in order to obtain the vertical adjustable range. The regression equation is

Seat Position Z = -252 + 0.99 H17 - 0.089 L11 - 0.037 Stature [22]

with RMSE = 20.8 mm.

Note that garb level does not affect the seat vertical position. Since stature is a significant predictor in the model, we proceed by calculating the mean and standard deviation of the vertical seat position for each gender.

$\mu_{seatpositionz,male}$ = -317 + 0.99 H17 - 0.089 $L11_{rel}$ [23]

$\mu_{seatpositionz,female}$ = -312.3 + 0.99 H17 - 0.089 $L11_{rel}$ [24]

$$\sigma_{seatpositionz,male} = \sqrt{(-0.037\sigma_{Stature,male})^2 + (20.8)^2} \quad [25]$$

$$\sigma_{seatpositionz,female} = \sqrt{(-0.037\sigma_{Stature,female})^2 + (20.8)^2} \quad [26]$$

The male and female distributions are combined in the same manner as for fore-aft seat position to obtain z_1 and z_2, respectively the lower and upper boundaries of the seat track.

In practice, a designer will likely want to accommodate a target percentage of drivers on fore-aft and vertical position simultaneously. Suppose the target is 95% accommodation on both vertical and fore-aft seat positions. To accommodate the central 95% of the population, the disaccommodation at the top, bottom, front, and back of a rectangular seat track must each be not more than approximately 1.3% (see Methods section for derivation).

Eyellipse

The fore-aft and vertical eye locations with respect to seat H-point are predicted using regression models given by

EyeReHPtX = 345 + 0.116 $L11_{rel}$ - 0.108 Stature -44 ln(BMI) R^2_{adj} = 0.08, RMSE = 40.1 [27]

EyeReHPtZ = -816 + 0.411 Stature + 29 ln(BMI) + 1262 SH/S R^2_{adj} = 0.77, RMSE = 17.3 [28]

Note that the fore-aft location of the eyes with respect to seat H-point is weakly related to body dimensions and steering wheel position, but vertical eye location relative to the seat is determined only by body dimensions. To obtain eye location with respect to the package origin (AHP), we must add the fore-aft and vertical mean seat positions to equations 27 and 28 to obtain male and female reference centroids for the eyellipse.

Garb effects are applied to the reference centroid. Relative to ACU, PPE shifts the reference centroid forward by 56.3 mm and upward by 13 mm. Relative to ACU, ENC shifts the reference centroid forward by 103 mm and upward by 13 mm.

The side-view angle of the eyellipse was computed by conducting a principal component analysis (PCA) on the side-view eye location data after centering the data from each condition, thereby removing package effects. The first principal component is calculated as (0.948, 0.319), so the x'-axis angle was computed as arctan(0.319/0.948) = 18.6 degrees. Note that this angle is not significantly affected by the anthropometric composition of the driver population across the range of interest.

The eye locations with respect to the x' and z' axes were regressed on the drivers' attributes, giving

x' = - 564 + 0.327 Stature , R^2_{adj} = 0.23, RMSE = 43.8 [29]

z' = - 1205 + 0.282 Stature + 1375 SH/S, R^2_{adj} = 0.42, RMSE = 28.7 [30]

Both the x' and z' coordinates were significantly related to drivers' attributes. Consequently, we use these relationships to calculate the cutoff points on each axis.

The centroid of the eyellipse is positioned with respect to the mean predicted seat position. Equations 29 and 30 are used with the mean population values of stature, *SH/S* and log(*BMI*) to obtain the mean seat position. The mean population value of stature is

$$\mu_{stature,pop} = m\mu_{stature,male} + (1-m)\mu_{stature,female} \quad [31]$$

where m is the fraction of the population that is male, $\mu_{stature,male}$ is the male mean stature and the female mean stature is represented by $\mu_{stature,female}$. The mean population value for *SH/S* is calculated similarly. An eyellipse reference centroid is then calculated with respect to the mean seat position using eye locations with respect to H-point with the mean anthropometric measures for the population. The reference centroid is used as a starting point to scale and locate the eyellipse, as follows:

1. Construct a side-view line passing through the reference centroid oriented at 18.6 degrees from horizontal (down at the front).

2. Find the male centroid by moving along the x' line relative to reference centroid by the distance given by

$$x'_{centroid,male} = 0.327\left(\mu_{stature,male} - \mu_{stature,pop}\right) \quad [32]$$

   where $\mu_{stature,pop}$ is the mean population stature. Similarly, find the female centroid by

$$x'_{centroid,female} = 0.327\left(\mu_{stature,female} - \mu_{stature,pop}\right) \quad [33]$$

3. Compute the standard deviation of eye location for male and female drivers along the *x*' axis from the standard deviations of stature by

$$s_{x',male} = \sqrt{\left(0.327 s_{stature,male}\right)^2 + \left(43.8\right)^2} \quad [34]$$

   and

$$s_{x',female} = \sqrt{\left(0.327 s_{stature,female}\right)^2 + \left(43.8\right)^2} \quad [35]$$

4. Choose the front axis point x'_1 such that a tangent to the ellipse at that point (perpendicular to *x'*) will cut off the desired fraction of the population by iteratively solving for x'_1 in $F_5 = m\varphi\left(\frac{x'_1 - x'_{centroid,male}}{\sigma_{x',male}}\right) + (1-m)\varphi\left(\frac{x'_1 - x'_{centroid,female}}{\sigma_{x',female}}\right)$ [36]

where φ is the cumulative standard normal distribution. Similarly, choose the rear axis point x'_2 to cut off the same fraction:

$$F_6 = m\left(1-\varphi\left(\frac{x'_2 - x'_{centroid,male}}{\sigma_{x',male}}\right)\right) + (1-m)\left(1-\varphi\left(\frac{x'_2 - x'_{centroid,female}}{\sigma_{x',female}}\right)\right) \quad [37]$$

The x' axis length is $x'_1 - x'_2$. The eyellipse centroid is located at $\frac{x'_1 + x'_2}{2}$. In general, this will be slightly displaced from the reference centroid location, because of differences between men and women in stature variance. The z' axis length can be computed analogous to the aforementioned procedure. Start by constructing the z' axis perpendicular to the x' axis through the reference centroid.

5. Compute the male and female z' centroids as

$$z'_{centroid,male} = 0.282\left(\mu_{stature,male} - \mu_{stature,pop}\right) + 1375\left(\mu_{SH/S,male} - \mu_{SH/S,pop}\right)$$
[38]

and

$$z'_{centroid,female} = 0.282\left(\mu_{stature,female} - \mu_{stature,pop}\right) + 1375\left(\mu_{SH/S,female} - \mu_{SH/S,pop}\right)$$
[39]

6. Compute the male and female standard deviation of eye locations along the z' axis

$$\sigma_{x',male} = \sqrt{\left(0.282\sigma_{stature,male}\right)^2 + \left(1375\sigma_{SH/S,male}\right)^2 + \left(28.73\right)^2} \quad [40]$$

and

$$\sigma_{x',female} = \sqrt{\left(0.282\sigma_{stature,female}\right)^2 + \left(1375\sigma_{SH/S,female}\right)^2 + \left(28.73\right)^2} \quad [41]$$

7. Calculating the cut off fraction on bottom of z' axis, we can acquire the cut off z'_1 point

$$F_7 = m\varphi\left(\frac{z'_1 - z'_{centroid,male}}{\sigma_{z',male}}\right) + (1-m)\varphi\left(\frac{z'_1 - z'_{centroid,female}}{\sigma_{z',female}}\right) \quad [42]$$

where φ is the cumulative standard normal distribution. The top cut off points can be obtained by cutting the same fraction as

$$F_8 = m\left(1-\varphi\left(\frac{z'_2 - z'_{centroid,male}}{\sigma_{z',male}}\right)\right) + (1-m)\left(1-\varphi\left(\frac{z'_2 - z'_{centroid,female}}{\sigma_{z',female}}\right)\right) \quad [43]$$

The z' length can be computed as $z'_1 - z'_2$.

Note that because we usually are constructing a cutoff ellipse (see Figure 4), the target fraction to cut off at each end of the x' and z' axes is identical. For example, to construct a 95% cutoff ellipse, the axes lengths are chosen to cut off 5% at each end. This differs from the construction of the seat track travel range, for which the goal is to *enclose* a target percentage of the population.

Note that the eyellipse size and orientation are the same for each package, given a particular population definition. Package variables (steering wheel position) affects the centroid location. Note that because the eyellipse is constructed from the mean seat position, all of the factors affecting mean seat position also affect eyellipse location.

To construct the rear view of the eyellipse, the lateral eye position is modeled. Lateral eye location is not affected by driver or vehicle attributes. Hence, we directly computed the mean and standard deviation of lateral eye locations with respect to AHP. By definition, the mean lateral head location is assumed to be on the driver centerline, so the centroids of the left and right eyellipses are each offset from the driver centerline by half the mean interpupillary breadth of 65 mm (i.e., ±32.5 mm) The standard deviation of lateral eye location is 14.8 mm. Since there is no significant correlation between the lateral and vertical eye locations (the eyellipse is not tilted in rear view), we calculate the eyellipse dimensions in the original YZ coordinates, without performing PCA. The lateral axis length of the eyellipse can be computed by solving the following equation

$$1 - C = \varphi\left(\frac{\frac{y}{2} - \mu_y}{\sigma_y}\right) \quad [44]$$

where *C* is the desired cutoff fraction (e.g., 0.95), φ is the cumulative standard normal distribution , mean lateral eye location with regard to driver centerline is $\mu_y = \pm 32.5$, the lateral eye location standard deviation is $\sigma_y = 14.8$, and the lateral axis length is *y*.

Helmet Contour

A cutoff contour for Soldiers wearing helmets was constructed using the methods from SAE J1052, using a standardized helmet contour rather than a head contour. The side- and rear-view helmet profiles relative to cyclopean eye were measured from laser-scan data. These profiles were then "spotted" around the eyellipses (placing the eye on the eyellipse boundary) to obtain the boundaries of the helmet contour envelope, which was then approximated by an ellipse.

Using scan data, we first approximated the side-view helmet contour using a Bezier curve with five control points. To obtain the appropriate positioning of the helmet contour with respect to the eye location, the helmet contour was translated to fit the means of top and back of head data measured in the driver mockup. First, the measured top-of-helmet and back-of-helmet points for Condition 5 were expressed relative to the eye location measured in the same condition. The helmet contour was then translated such that the top and back of the contour matched the means of the measured top- and back-of-helmet points. In this way, the Soldier's preferred helmet locations relative to their eye locations were captured. Points defining the contour relative to eye and driver centerline are listed in Appendix B.

Next, the helmet profile relative to eye location was translated around the eyellipse. To efficiently use all the observations (both PPE and ENC data), we centered helmet point data from all trials with helmets at the eye location measured in each trial. The helmet profile was positioned at 100 evenly spaced points on the top of the eyellipse. Approximately 5 percent (16 of 275 = 5.8%) of the measured helmet points lay outside the top or back of the translated contours for this 95% cutoff eyellipse, confirming the suitability of the J1052 method for these data. (Exact correspondence with the nominal 5% cutoff is not expected, given the random character of the sample population.)

Using the dimensions of the eyellipse, combined with the contour of the helmet with respect to the eye location, we can calculate the bounds for the helmet contour. Specifically, we want the offsets relative to the eyellipse that result from placing the eye location of the helmet contour at the most forward, highest, and most rearward points on the eyellipse. Referring to the data in Appendix B, the most forward point on the sideview contour is -52.2 mm forward of the eye; the highest point is 161.8 mm above the eye; and the most rearward is 217 rearward of the eye.

Next, we must find the most forward, highest, and most rearward points on the eyellipse. Assuming that the eyellipse is centered on the origin, the equation of the ellipse in side view is given by

$$A\,x^2 + B\,x\,z + Cz^2 = 1 \qquad [45]$$

where

$$A = \left(\frac{\cos\theta}{a}\right)^2 + \left(\frac{\sin\theta}{b}\right)^2 \qquad [46]$$

$$B = 2\,cos\theta\,sin\theta\,\left(\frac{1}{a^2} - \frac{1}{b^2}\right) \qquad [47]$$

$$C = \left(\frac{\sin\theta}{a}\right)^2 + \left(\frac{\cos\theta}{b}\right)^2 \qquad [48]$$

and a is the length of the x' axis, b is the length of the z' axis, and θ is the angle of the x' axis with respect to the global x axis (18.6 degrees).

To find the highest point on the ellipse, we solve the quadratic for y,

$$z = \frac{-Bx + \sqrt{4C + B^2x^2 - 4AC\,x^2}}{2C} \qquad [49]$$

differentiate with respect to x, set the expression equal to zero, and solve for x, yielding

$$x_{zmax} = \frac{-B}{\sqrt{A}\sqrt{4AC - B^2}} \qquad [50]$$

Inserting x_{zmax} into the expression for z gives the coordinates of the highest point. Similarly, we can find the front and rear points using

$$x = \frac{-Bz \pm \sqrt{4A + B^2z^2 - 4AC\,z^2}}{2A} \qquad [51]$$

and

$$z_{xmax} = \frac{-B}{\sqrt{C}\sqrt{4AC - B^2}} \qquad [52]$$

Applying the helmet margins to these coordinates defines the front, top, and rear of a bounding box for the helmet contour ellipse. Because the convex hull of the helmet contours is not a true ellipse, determining the centroid location requires a heuristic formula. A good approximating contour can be obtained for typical populations using a centroid located 61.4 mm above and 82.4 mm rearward of the eyellipse centroid.

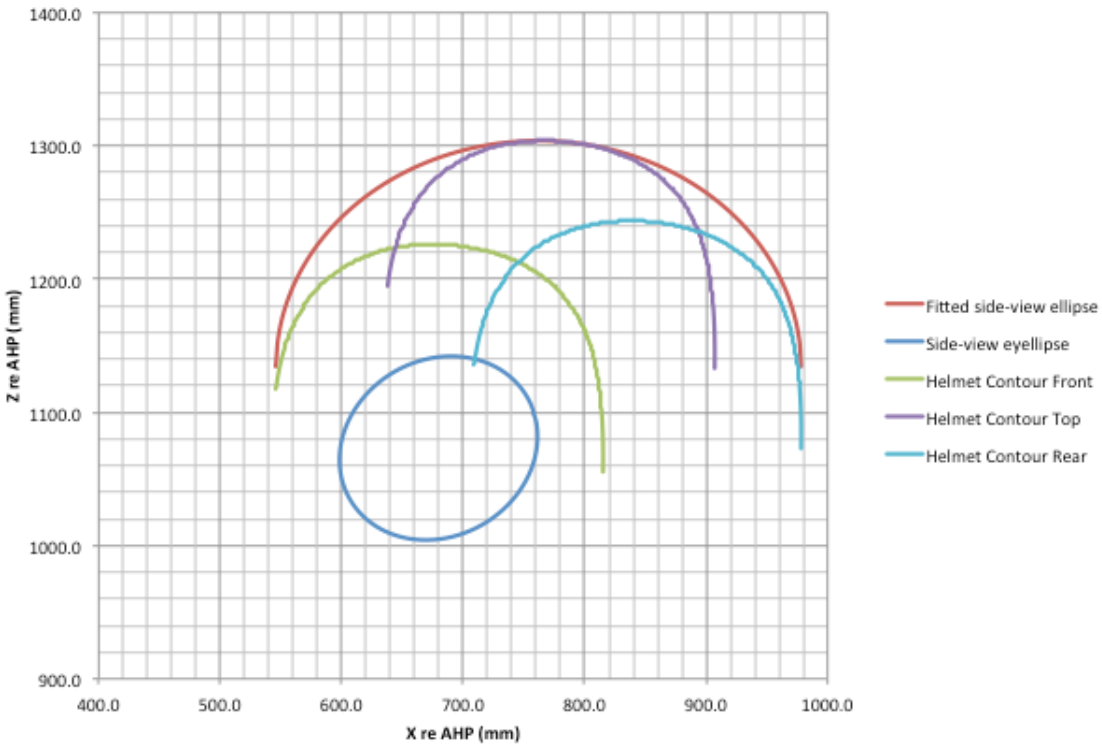

Figure 6. Fitted **side-view** driver helmet ellipse with eyellipse and helmet profiles positioned relative to the front, top, and rear of eyellipse.

For rear view, the head contour is constructed with two elliptical sections joined by a flat section at the top. Given that the height of the top of the contour is already specified by the side view construction, we need only find the breadth relative to the side of eyellipse. Relative to the head centerline, the helmet extends 129 mm laterally. The additional clearance requirement due to variance in lateral head position is given by the eyellipse Y-axis length. Because the helmet has a nearly flat contour on the top, a better approximation of the clearance requirement is obtained by generating separate ellipsoid profiles for the left and right sides, using the eye centerlines (±32.5 mm from occupant centerline) as the contour ellipsoid lateral coordinate. The vertical helmet contour centroid coordinate has already been determined in side view. Hence, the (half) axis length for the rear-view helmet contour is 129 mm plus half the eyellipse lateral axis length. Figure 7 shows the rear-view helmet contour segments along with translated helmet profiles.

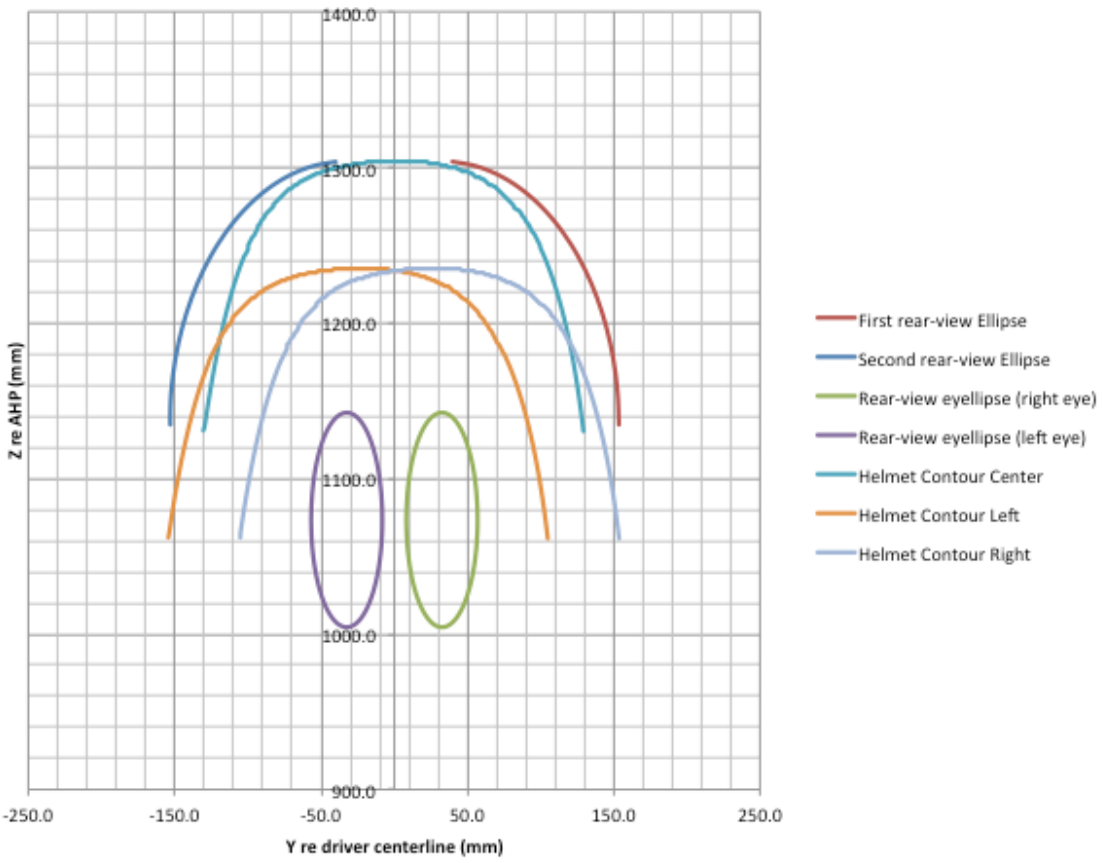

Figure 7. Fitted **rear-view** driver helmet ellipse with eyellipse and helmet profiles positioned relative to the left, top, and right of eyellipse.

For three-dimensional applications, the helmet contour can be created by first generating an ellipsoid aligned to grid with the X and Z axis lengths given by the side-view calculations. The lateral axis length is 129 mm plus half the eyellipse lateral axis length. The bottom half of the ellipsoid is removed. The remainder is split along the driver centerline and the sides offset ±32.5 mm laterally. These sections can be extruded horizontally to the centerline to create a continuous contour.

The SAE J1052 contour includes a 23-mm outward shift of the outboard half of the contour to account for the space required for head turn. Although data specific to soldiers on spatial requirements for head turn are not available, we recommend modifying the current contour in the same way. After constructing the contour, section the contour on vertical plane at the occupant centerline, shift the outboard half outboard by 23 mm, and fill the gap.

Knee Contour

A knee cutoff contour was modeled for the right knee in the normal driving position using methods reported in Reed (2006). Note that the contours can be reflected around driver centerline to model the left knee. The location of the suprapatella landmark at the upper, forward margin of the right patella was recorded for each driver in a normal driving posture with the right foot on the accelerator pedal. Using regression analysis, we developed a statistical model predicting the suprapatella location based on the anthropometric features of the drivers and some vehicle design variables. To account for knee width, we expanded the models laterally 110 mm, the average knee breadth in these data. The location of the top of the shin is estimated by translating the suprapatella ellipse down and forward. The magnitude of the translation is based on measurements of knee geometry reported in Reed (2006) and the direction is based on a predicted leg segment angle. Additional clearance lines are constructed representing the shin and the top of the thigh.

Suprapatella Landmark Locations – Three coordinate values were modeled:

PatellaX: Fore-aft location of the suprapatella landmark relative to seat H-point.

PatellaY: Lateral location of the suprapatella landmark relative to driver centerline.

PatellaZ: Vertical location of the suprapatella landmark above AHP.

Table 6 shows the regression models for the ACU condition. The fore-aft (X) location of the patella was predicted relative to seat H-point as a function of vertical steering wheel position relative to AHP, stature, ratio of sitting height to stature and the natural log of body mass index (BMI). (The log-transformed BMI better approximates a normal distribution than does the untransformed BMI for typical populations.) PPE and ENC shift the hips, and hence knees, forward relative to the seat H-point. The forward shifts are 23 and 47 mm for PPE and ENC (rifleman) levels, respectively. These are subtracted from the PatellaX value given in Table 6.

Table 6
Regression Models for Predicting Knee Locations (ACU)

Dependent Measure	Constant	H17	L11rel	Stature	ln(BMI)	SH/S	R^2_{adj}	RMSE
PatellaX	-79.3	-0.225	-	-0.151	-21.4	258	0.336	21.95
PatellaY	-395	-	-0.0842	0.217	61.5	-	0.336	26.54
PatellaZ	9.6	0.412	-0.219	0.289	0	-543	0.779	17.3

Predicting relative to seat H-point rather than AHP allows the effects of the vehicle package on fore-aft seat position to be taken into account through application of the seating accommodation model. The R^2 value for predicting the patella location forward of seat H-point is only 0.36, indicating a modest level of predictive ability for the model. The lateral patella location relative to driver centerline is predicted by stature, BMI and the relative fore-aft steering wheel position with regard to AHP. The vertical knee location can be predicted by the vertical and fore-aft steering wheel positions, stature and the ratio of sitting height to stature. The values in the root-mean square error (RMSE) column in Table 6 quantify the residual variance in knee location that is not accounted for by the predictors. This variance is important in estimating the distribution of knee locations for a population of drivers.

A cutoff ellipsoid for the suprapatella location is calculated as follows:

1. Obtain the horizontal, lateral and vertical mean knee locations for both men and women using the models presented in Table 6.

2. Compute the standard deviation of fore-aft knee location as

$$s_{PatellaX} = \sqrt{(-0.151 s_{Stature})^2 + (-21.4 s_{\ln(BMI)})^2 + (258 s_{SH/S})^2 + (21.95)^2} \quad [53]$$

The mean knee location with regard to AHP can be obtained by adding the mean horizontal knee location relative to H-point to the mean seat position with respect to AHP. Hence, the standard deviation of the horizontal knee location relative to AHP is

$$\sigma_{PatellaXrtAHP} = \sqrt{(\sigma_{seatpositionx})^2 + (\sigma_{PatellaX})^2 + 2\rho\sigma_{seatpositionx}\sigma_{PatellaX}} \quad [54]$$

where $s_{PatellaXrtAHP}$ is the standard deviation of the fore-aft knee location relative to AHP, $s_{seatpositionx}$ is the standard deviation of the seat position with regard to AHP, $s_{PatellaX}$ is the standard deviation of fore-aft knee location relative to H-point, and ρ is the correlation between horizontal knee location and fore-aft seat position, which was calculated as –0.61. The lateral knee location standard deviation is given by

$$s_{PatellaY} = \sqrt{(0.217 s_{Stature})^2 + (61.5 s_{\ln(BMI)})^2 + (26.54)^2} \quad [55]$$

Similarly, the standard deviation of the vertical knee location relative to AHP is

$$s_{PatellaZ} = \sqrt{(0.289 s_{Stature})^2 + (-543 s_{SH/S})^2 + (17.3)^2} \quad [56]$$

3. The weighted mean knee location for the two-gender population is

$$\mu_{w,patella} = m\mu_{patella,male} + (1-m)\mu_{patella,female} \quad [57]$$

where m is the male fraction in the population, $\mu_{w,patella}$ represents the weighted mean locations, and $\mu_{patella,male}$ and $\mu_{patella,female}$ are the male and female mean knee locations respectively.

4. The x, y, and z axis lengths x_1 , y_1, and z_1 are chosen such that a tangent to the ellipse at that point (perpendicular to the axes) will cut off the desired fraction of the population by iteratively solving for x_1 , y_1 and z_1 in

$$1-C = m\varphi\left(\frac{\left(\mu_{w,patella} - \frac{x_1}{2} - \mu_{patella,male}\right)}{\sigma_{patella,male}}\right) + (1-m)\varphi\left(\frac{\left(\mu_{w,patella} - \frac{x_1}{2} - \mu_{patella,female}\right)}{\sigma_{patella,female}}\right)$$

[58]

where C is the desired ellipse cutoff (e.g., 95%), m is the male fraction in the population, φ is the cumulative standard normal distribution, the weighted mean locations is denoted by $\mu_{w,patella}$, $\mu_{patella,male}$ and $\mu_{patella,female}$ are the male and female mean knee locations respectively, and $\sigma_{patella,male}$ and $\sigma_{patella,female}$ denote the male and female knee location standard deviations correspondingly.

5. During construction of the ellipsoid, the lateral dimension is expanded by 110 mm to account for knee breadth.

Top of Shin — The suprapatella landmark ellipsoid provides a guide for clearance at the top of the knee. To obtain the clearance at the top of the shin, the suprapatella ellipsoid is translated down and forward. The angle of the translation is dependent on the leg segment angle (angle of the vector from the right ankle joint to the right knee joint in side view with respect to vertical). A regression analysis gives:

Leg Segment Angle (deg) = 107 – 0.106 H17 + 0.0612 L11rel, R^2 = 0.60, RMSE = 4.7 [59]

With the leg segment vertical, the translation from the suprapatella to shin point is 22.7 mm forward, 47.1 mm downward (Reed 2006). This vector is rotated by the magnitude of the leg segment angle to give the appropriate translation.

Knee Contour — A new knee contour ellipsoid spanning the suprapatella and top of shin ellipsoids is constructed such that the top of the knee contour has the same Z coordinate as the top of the suprapatella ellipsoid and the front of the knee contour has the same X coordinate as the front of the top-of-shin contour.

Shin and Thigh Clearance Lines — A 200-mm-long shin clearance line is constructed downward tangent to the front of the knee contour at the leg segment angle. A thigh clearance line is constructed rearward tangent to the top portion of the knee contour at the thigh segment angle given by:

Thigh Segment Angle (deg) = 12 – 0.087 H17 + 0.0358 WMS, R^2 = 0.55, RMSE = 4.0 [60]

where WMS is the mean stature weighted by the male/female fraction:

$$WMS = m\eta_{stature,male} + (1- m)\eta_{stature,female} \qquad [61]$$

Figure 8 shows the knee contour construction in side view. Note that only the forward and upper edge of the contour has meaning for design. The lower and rearward surfaces do not have meaningful anatomical referents. For example, the bottom of the contour does not represent clearance under the knee.

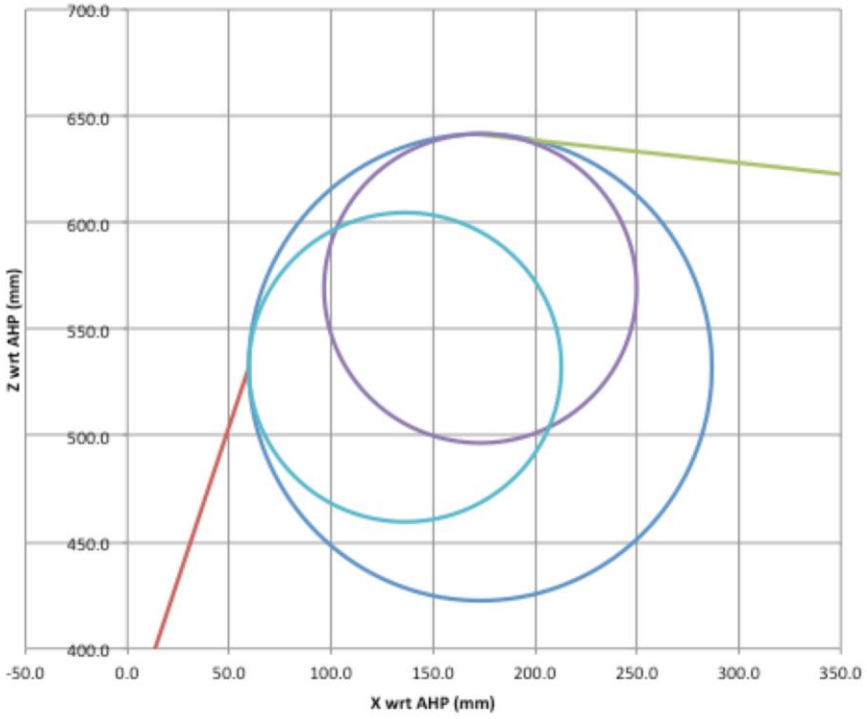

Figure 8. Knee contour construction.

Torso Contour

Clearance between the torso and the steering wheel is an important consideration, particularly when drivers are wearing body armor or body-borne gear. During the driver trials in the Seated Soldier Study, the location of the IOTV and ENC (Rifleman) gear set were measured at several reference points. For the current analysis, simplified versions of the side-view and top-view contours were created and

positioned based on the measured data, using a method similar to that used for the knee clearance contours.

Creating the Contours – In each IOTV and ENC trial, 3 reference points on the vest or gear were recorded. The clearance contour is created by (1) generating average top- and side-view contours relative to one reference point and (2) creating a positioning model for the reference point based on a regression analysis. As with the eyellipse and head contour, the torso contour is positioned relative to mean seat position.

Because each Soldier sat with a slightly different torso orientation, a contour that accounted for these variations relative to the reference point location was needed. For the IOTV, a low-resolution contour of the front of the size-large IOTV was positioned relative to the measured reference point locations for each trial. Profiles were created in side-view and top-view by taking the convex hull of the resulting contour points. These contours were centered on one reference point location to be used in positioning the contours. A similar procedure was used for the ENC (rifleman) condition to obtain side- and top-view contours.

A regression analysis was conducted to predict the reference point location with respect to seat position (translated H-point) as a function of vehicle and driver variables. Table 7 lists the positioning models. Note that the reference point was chosen for convenience of measurement does not correspond to any particular aspect of the torso contour.

The model predictions are generated as follows:

1. The mean reference point location within gender is predicted and added to the mean seat position for each gender to establish the mean reference point location in package space.
2. The standard deviation of the fore-aft position of the contour is calculated, including the residual variance from the regression predicting the reference point location with respect to seat position, the variance in seat position for each gender, and the covariance between seat position and the reference point location.
3. The desired cutoff quantile at the front of the distribution is computed from the two single-gender distributions as with the seat position calculations.
4. The vertical position of the ENC contour relative to seat position was not significantly affected by any predictors; consequently, a fixed vertical offset from mean seat position is used. However, the IOTV contour location was significantly affected by several variables, notably the ratio of sitting height to stature (SH/S).

Table 7
Locating Equations Relative to Mean Seat H-Point for Torso Contour Reference Points

Reference Point	Constant	Stature	Ln(BMI)	SH/S	R^2_{adj}	RMSE	Correlation with Seat Position
IOTV-X	-215		92.9		0.23	25.1	-0.18
IOTV-Z	-408	0.156	119	349	0.71	13.3	
ENC-X	188.8	-0.095	75.2		0.13	31.7	-0.4
ENC-Z	299						

The torso contours relative to the reference points are listed in Appendix C. Figure 9 shows the side- and top-view torso contours for the ANSUR population. Note that the contours are affected by vehicle geometry only through the mean seat position prediction.

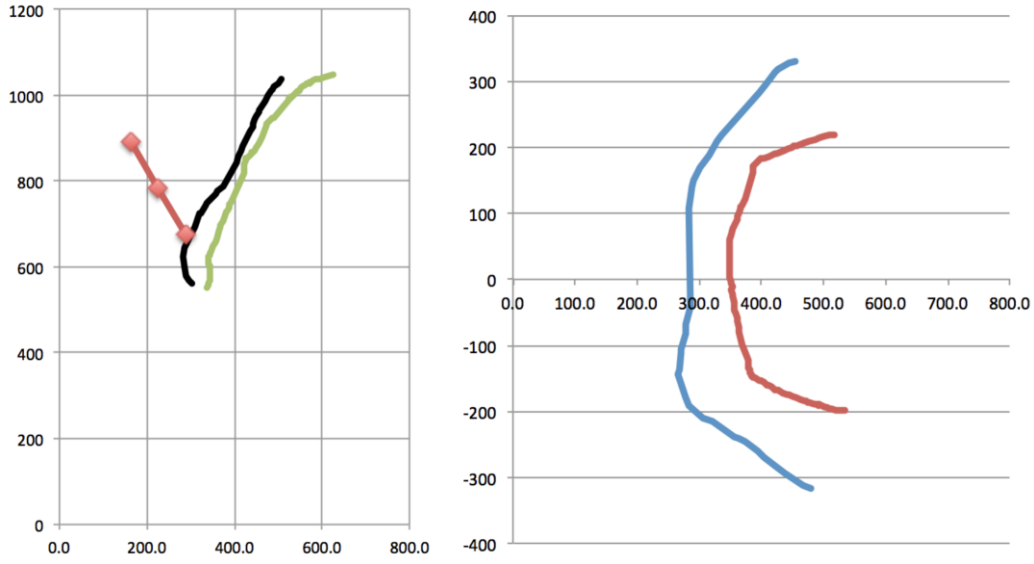

Figure 9. Illustration of 95%-cutoff torso contours in sideview (left) and top view (right) relative to AHP and driver centerline. In each figure, the ENC (rifleman) contour is further forward (to the left) and the IOTV contour is further rearward.

Driver Preference for Steering Wheel Location

In the Seated Soldier Study, the steering wheel location was fixed, so the data do not include information about driver preference for steering wheel location. Nonetheless, locating the steering wheel is an important part of vehicle packaging, so some guidance is desired. In a previous study of truck driver postures, drivers adjusted to the steering-wheel-to-pedal relationship from a range of starting positions (Reed 2005). These data were used to develop a steering-wheel locator model based on driver posture. To determine whether the model would be applicable to military vehicles, postures measured in the Seated Soldier Study were

compared with postures measured in the previous work with truck drivers. If the relative positions of the seat and steering wheel were similar, then the steering wheel preference model is likely to be applicable. The analysis showed that seat positions predicted by the truck driver models for the range of steering wheel positions used in the Seated Soldier Study were similar to those observed with Soldiers, indicating that Soldiers and truck drivers prefer similar steering wheel locations. Consequently, the truck driver model is reproduced here for application to military vehicles.

Analysis of driver preference data showed that the preferred driver steering wheel height (H17) for an L11 value of 175 mm was a significant function of stature:

$$SWPrefHt@175 \text{ (mm)} = 524 + 0.1613\ Stature,\ R^2 = 0.32,\ RMSE = 23.4 \quad [62]$$

The average slope of the preference line is -0.559 (s.d. 0.305). Combining these, the steering wheel preference line is given by

$$SWPrefHt \text{ (mm)} = 524 + 0.1613\ Stature - 0.559\ (x - 175) \quad [63]$$

where x is the distance aft of AHP.

For purposes of the new accommodation models, the location of an adjustable steering wheel is chosen with respect to the steering wheel preference line. First, the geometric center (centroid) of the travel envelope for the center of the steering wheel in side view is calculated. (The center of the wheel is defined, as in SAE J1100, as the intersection between the axis of rotation of the wheel and a plane lying on the driver side of the wheel.) Next, the point on the steering wheel preference line that is closest to the geometric center of the travel envelope is calculated. If this point lies within the travel envelope, it is used as the steering wheel location to define Ll1 and H17 for input to the models. If the closest point on the preference line to the travel-envelope centroid lies outside the travel envelope, the point of intersection between the travel envelope and the perpendicular line from the preference line to the centroid is used. Figure 9 shows the calculation schematically. This approach provides an objective, data-based method for representing the effects of adjustable steering wheels on driver posture, while also providing some design guidance.

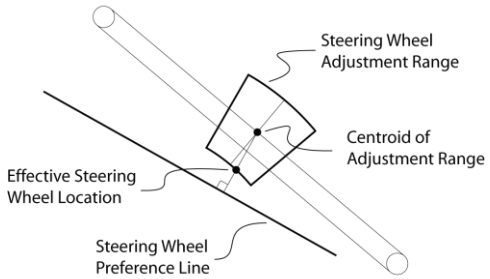

Figure 9. Calculating effective steering wheel location for a case in which the preference line does not pass through the adjustment range.

Use of Seat Index Point Tool

The models presented above are based on the seat H-point measured using the SAE J826 H-point manikin and procedures. Recent research has shown that the ISO 5353 Seat Index Point Tool (SIPT) can be used as an alternative measurement tool if the J826 manikin is not available (Reed and Ebert, 2014). Across a wide range of seating conditions, the seat index point (SIP) was on average 5 mm rearward of the J826 H-point. Consequently, an estimated H-point for use with these models can be generated by translating the SIP forward by 5 mm relative to the seat.

DISCUSSION

This report presents accommodation models for Soldiers as drivers. The modeling methodology follows the state-of-the-art techniques developed for passenger cars and light trucks (Flannagan et al. 1998, Manary et al. 1998) and previously applied to the development of similar models for commercial truck drivers (Reed 2005, Reed 2006). These are the first accommodation models based on Soldier data and the first to include the effects of PPE and body borne gear.

Although the models are specifically intended for driving scenarios with fixed pedals and steering wheel, the results embody a general description of Soldier-selected postures that could be extended to other situations. The driver models represent combinations of foot, hand, hip, and head locations that soldiers have found to be comfortable. These could be applied with confidence to laying out other workstations that require primarily horizontally directed vision in a seating scenario with an adjustable seat and a hand task. However, important differences in task demands should be considered. For example, a commander workstation adjacent to the driver would not necessarily need the same level of seat position adjustment. Yet, designing with the driver models, using communications or other controls as the hand task input, would provide confidence that sufficient accommodation was available.

The most important limitation of the driver models is that they have not been validated through in-vehicle testing. In particular, some effects of vehicle geometry and the nature of the driving task could result in differences in driver posture. Exterior vision obstructions could result in posture differences. Conceptually, a very small windshield opening could constrain driver eye locations to lie with a smaller or different area than that predicted by the eyellipse models in this report. However, previous research with passenger car drivers has shown that even substantial vision restrictions have only small effects on posture (Reed et al. 2003b). In research with commercial truck drivers, accommodation models created from laboratory data were accurate in predicting the distribution of driver postures in trucks with widely varying exterior vision restrictions (Reed et al. 2005). However, for military applications, accommodation models for situations with highly constrained eye locations will be needed.

The driver accommodation models in this report also do not take into account the effects of censoring of posture due to restrictions in cab space or seat adjustment ranges. For example, headroom restrictions could cause drivers to sit lower than predicted. The seating accommodation model assumes that drivers can sit with their preferred seat position and seat back angle. If the seat adjustments are restricted, the postures may be different.

The models are limited by the particular uniform and gear conditions that were used in data collection. The ACU condition included standard-issue boots with an effective heel height of about 25 mm. Boots with thicker heels would be expected to

have a small effect on posture, roughly equivalent to the same increase in stature. More importantly, the PPE and ENC conditions were based on particular garb configurations. The IOTV and ACH geometry had a significant effect on soldier posture and space claim. The effects of a different helmet (or the additional of helmet-mounted equipment) could be accounted for by amending the helmet contour model. However, the effects of a change in body armor or the configuration of the body borne gear would need to be investigated through additional posture measurements. One important limitation of the ENC conditions is that that a single hydration pack was used. Soldiers not wearing a hydration pack or sitting on a seat with an opening designed to accommodate the hydration pack would be expected to sit somewhat differently. Although new data would be the best way to account for different seats, using the PPE models for ENC situations with hydration pack relief is a reasonable approach.

The data on which these models are based were gathered from a convenience sample of Soldiers at three Army posts in 2012, but this does not impose a substantial limitation. Because the modeling methodology is not strongly dependent on the representativeness of the sample, even relatively large changes in the anthropometric distributions of Soldiers would not have important effects on the validity of these models. However, large changes in the nature of the driving task and the associated changes in vehicle design would make these models less useful. For example, drivers using on-head displays for forward vision might position themselves differently. Similarly, highly adjustable steering wheels and pedals might result in different seat position adjustment behavior.

REFERENCES

Dempster, W.T. (1955). Space requirements of the seated operator: Geometrical, kinematic, and mechanical aspects of the body with special reference to the limbs. WADC Technical Report No. 55-159. Wright-Patterson Air Force Base, OH: Wright Air Development Center.

Flannagan, C.A.C., Manary, M.A., Schneider, L.W., and Reed, M.P. (1998). An Improved seating accommodation model with application to different user populations. *SAE Transactions: Journal of Passenger Cars,* 107(6): 1189-1197.

Geoffrey, S.P. (1961). A 2-D Manikin –the Inside Story. SAE Technical Paper 267A. Society of Automotive Engineers, Warrendale, PA.

Gordon CC, Churchill T, Clauser CE, Bradtmiller B, McConville JT, Tebbetts I, and Walker RA (1989) *1988 Anthropometric Survey of U.S. Army Personnel: Methods and Summary Statistics*. NATICK/TR-89/044. U.S. Army Natick Soldier Research, Development, and Engineering Center, Natick, MA.

Hammond, D.C. and Roe, R.W. (1972). SAE controls reach study. Technical Paper 720199. Warrendale, PA: Society of Automotive Engineers, Inc.

Jahns, S.K., Reed, M.P., and Hardee, H.L. (2001). Methods for in-vehicle measurement of truck driver postures. SAE Technical Paper 2001-01-2821. Society of Automotive Engineers, Warrendale, PA.

Meldrum, J.F. (1965). Automobile driver eye position. Technical Paper 650464. Warrendale, PA: Society of Automotive Engineers, Inc.

Manary, M.A., Flannagan, C.A.C., Reed, M.P., and Schneider, L.W. (1998). Development of an improved driver eye position model. *SAE Transactions: Journal of Passenger Cars,* 107(6): 43-50.

Paquette SP, Gordon CC, and Bradtmiller B (2009) *ANSUR II Pilot Study: Methods and Summary Statistics*. NATICK/TR-09/014. U.S. Army Natick Soldier Research, Development, and Engineering Center, Natick, MA.

Phillipart, N.L., Kuechenmeister, T.J., and Stanick, J.M. (1985). Describing the truck driver workspace. Technical Paper 85217. Warrendale, PA: Society of Automotive Engineers, Inc.

Reed, M.P., Manary, M.A., and Schneider, L.W. (1999). Methods for measuring and representing automobile occupant posture. Technical Paper 990959. Society of Automotive Engineers, Warrendale, PA.

Reed, M.P., Lehto, M.M., and Schneider, L.W. (2000a). Methods for laboratory investigation of truck and bus driver postures. Technical Paper 2000-01-3405. *SAE Transactions: Journal of Commercial Vehicles, Vol. 109*.

Reed, M.P., Manary, M.A., and Schneider, L.W. (2000b). The effects of forward vision restriction on automobile driver posture. *Transportation Human Factors,* 2(2). 173-179.

Reed, M.P. and Flannagan, C.A.C. (2000c). Anthropometric and postural variability: limitation of the boundary manikin approach. Technical Paper 2000-01-2172. Warrendale, PA: Society of Automotive Engineers, Inc.

Reed, M.P. (2005). Development of a New Eyellipse and Seating Accommodation Model for Trucks and Buses. Technical Report UMTRI-2005-30. University of Michigan Transportation Research Institute, Ann Arbor, MI.

Reed, M.P. (2006). Accommodation Models for Truck Driver Knee Clearance, Abdomen Clearance, and Shifter Location. Technical Report UMTRI-2006-30. University of Michigan Transportation Research Institute, Ann Arbor, MI.

Reed, M.P. and Ebert, S.M. (2013). The Seated Soldier Study: Posture and Body Shape in Vehicle Seats. Technical Report 2013-13. University of Michigan Transportation Research Institute, Ann Arbor, MI.

Reed, M.P., and Ebert, S.M. (2014). Evaluation of the Seat Index Point Tool for Military Seats. Technical Report UMTRI-2014-33. University of Michigan Transportation Research Institute, Ann Arbor, MI.

Sanders, M.S. and Shaw, B.E. (1985) U.S. truck driver anthropometric and truck work space data survey: sample selection and methodology. Technical Paper 852315. Warrendale, PA: Society of Automotive Engineers, Inc.

SAE International (2013). *SAE Handbook.* Warrendale, PA: Society of Automotive Engineers, Inc.

Stanick, J.M., Phillipart, N.J., and Kuechenmeister, T.J. (1987). Describing the truck driver eye and head accommodation. Technical Paper 871531. Warrendale, PA: Society of Automotive Engineers, Inc.

APPENDIX A

EXAMPLE CALCULATIONS

All dimensions in mm unless otherwise noted.

ANSUR II (2013)

Dimension	**Men**		**Women**	
	Mean	SD	Mean	SD
Stature (S), mm	1756	68.6	1628	64.2
Erect Sitting Height (SH), mm	918	35.7	857	33.1
Stature minus Sitting Height (SSH), mm	837	46.5	772	44.4
SH/S, --	0.523	0.0135	0.526	0.0141
Log(BMI)*, log(kg/m^2)	3.31	0.146	3.23	0.135

*Note -- this is natural log of BMI. In Excel, use = LN(BMI)

Fraction Male 0.9

Vehicle Geometry

SWX (L11)	337.5	mm
SWZ (H17)	735	mm
L11rel	0	
A40	0	mm
H30	423	mm
Ensemble Level	PPE	ACU, PPE, ENC
Hydration Pack Relief	No	Yes, No
Calibration Tool	J826	J826, SIPT

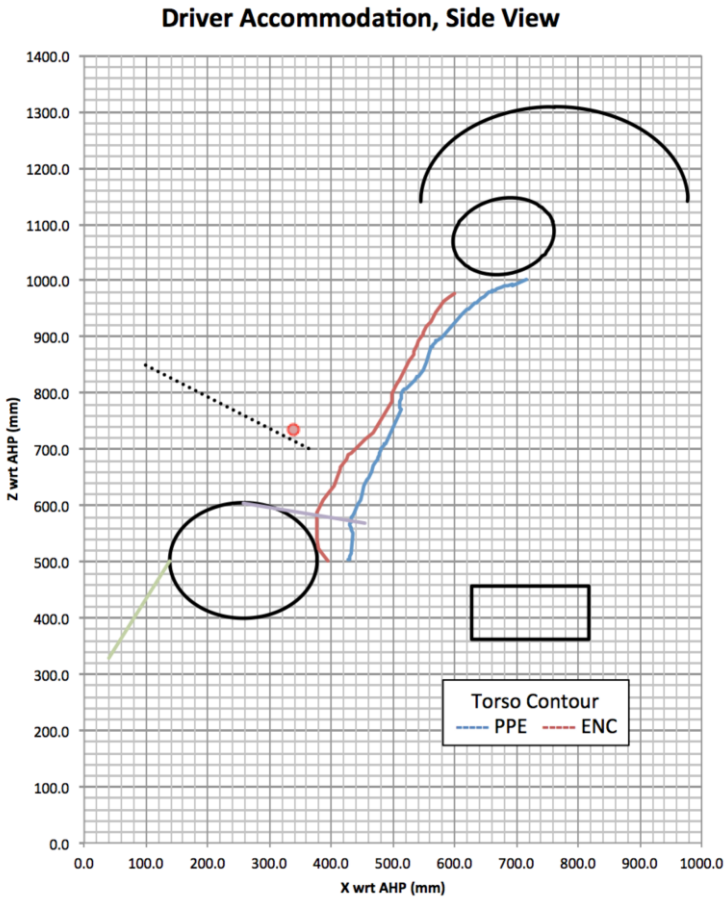

Figure A1. Overview of outputs.

Steering Wheel Preference

	L11 (mm)	H17 (mm)
Preference Line Endpoint, Min	363.2	700.0
Preference Line Endpoint, Max	94.8	850.0
Steering Wheel Point (SWP)	337.5	735.0

Seating Accommodation

Center of Travel (X)	721.6	mm
Center of Travel (Z)	408.7	mm
Fore-Aft Travel (X)	190.9	mm
Vertical Travel (Z)	93.9	mm

	X (mm)	Z (mm)
Full Down, Full Rear	817.1	361.7
Full Down, Full Forward	626.2	361.7
Full Up, Full Forward	626.2	455.6
Full Up, Full Rear	817.1	455.6
Full Down, Full Rear	817.1	361.7

SEAT BACK ANGLE (deg) PREFERENCE		
Front of Range	15.5	deg
Rear of Range	27.7	deg

Eyellipse

Eyellipse Centroids	X (mm)	Y (mm)	Z (mm)
Right	678.9	32.5	1078.1
Left	678.9	-32.5	1078.1

Side View of Eyellipses (X, Z)		
Eyellipse Angle (X' Axis wrt Horizontal)	18.6	deg
Axis Length (X')	166.9	mm
Axis Length (Z')	133.0	mm

Rear View of Eyellipses (Y, Z)		
Axis Length (Y)	48.7	mm
Axis Length (Z)	136.8	mm

Helmet Contour

Construction Centroids	X (mm)	Y (mm)	Z (mm)
Right	761.3	32.5	1139.5
Left	761.3	-55.5	1139.5

Side View of Helmet Contour (X, Z)		
Axis Length (X)	432.9	mm
Axis Length (Z)	337.6	mm

Rear View of Helmet Contour (Y, Z)		
Axis Length (Y)	241.7	mm
Axis Length (Z)	337.6	mm

Knee Contour

Knee Centroids	X (mm)	Y (mm)	Z (mm)
Right	257.7	186.3	501.9
Left	257.7	-186.3	501.9

Side View of Knee Contours (X, Z)		
Axis Length (X)	238.8	mm
Axis Length (Z)	205.4	mm

Rear View of Knee Contours (Y, Z)		
Axis Length (Y)	267.5	mm
Axis Length (Z)	205.4	mm

Torso Contour

Mean Reference Point	X (mm)	Z (mm)
PPE	566.6	848.2
ENC	389.7	707.7

APPENDIX B

HELMET CONTOURS

Sagittal		Coronal	
X	Z	Y	Z
-52.2	53.4	-129.9	-11.0
-51.8	56.7	-129.0	-5.3
-51.2	60.0	-128.1	0.2
-50.6	63.3	-127.2	5.7
-50.0	66.4	-126.3	10.9
-49.3	69.5	-125.4	16.1
-48.6	72.5	-124.5	21.1
-47.8	75.5	-123.5	25.9
-47.0	78.4	-122.6	30.6
-46.1	81.2	-121.7	35.2
-45.2	83.9	-120.7	39.7
-44.3	86.6	-119.8	44.0
-43.3	89.2	-118.8	48.2
-42.3	91.8	-117.9	52.3
-41.3	94.3	-116.9	56.3
-40.2	96.7	-115.9	60.1
-39.0	99.1	-114.9	63.8
-37.9	101.4	-113.9	67.5
-36.7	103.7	-112.9	71.0
-35.4	105.9	-111.9	74.4
-34.2	108.1	-110.9	77.7
-32.9	110.2	-109.9	80.9
-31.5	112.2	-108.9	84.0
-30.2	114.2	-107.8	87.0
-28.8	116.2	-106.8	89.9
-27.3	118.0	-105.8	92.8
-25.9	119.9	-104.7	95.5
-24.4	121.7	-103.6	98.1
-22.9	123.4	-102.6	100.7
-21.3	125.1	-101.5	103.2
-19.8	126.7	-100.4	105.6
-18.2	128.3	-99.3	107.9
-16.6	129.9	-98.2	110.1
-14.9	131.4	-97.1	112.3
-13.3	132.8	-96.0	114.4
-11.6	134.2	-94.8	116.4
-9.9	135.6	-93.7	118.3
-8.2	136.9	-92.6	120.2
-6.4	138.2	-91.4	122.0
-4.6	139.5	-90.3	123.7

-2.9	140.7	-89.1	125.4
-1.0	141.8	-87.9	127.1
0.8	143.0	-86.8	128.6
2.6	144.0	-85.6	130.1
4.5	145.1	-84.4	131.6
6.4	146.1	-83.2	133.0
8.2	147.1	-82.0	134.3
10.2	148.0	-80.7	135.6
12.1	148.9	-79.5	136.9
14.0	149.8	-78.3	138.0
16.0	150.6	-77.0	139.2
17.9	151.4	-75.8	140.3
19.9	152.2	-74.5	141.4
21.9	152.9	-73.3	142.4
23.9	153.6	-72.0	143.4
25.9	154.3	-70.7	144.3
27.9	154.9	-69.4	145.2
29.9	155.5	-68.1	146.1
31.9	156.1	-66.8	146.9
34.0	156.6	-65.5	147.7
36.0	157.1	-64.2	148.5
38.1	157.6	-62.9	149.2
40.1	158.1	-61.5	149.9
42.2	158.5	-60.2	150.6
44.2	158.9	-58.9	151.2
46.3	159.3	-57.5	151.8
48.4	159.6	-56.2	152.4
50.5	159.9	-54.8	152.9
52.5	160.2	-53.4	153.5
54.6	160.5	-52.0	154.0
56.7	160.7	-50.6	154.5
58.8	160.9	-49.3	155.0
60.9	161.1	-47.9	155.4
63.0	161.3	-46.4	155.8
65.1	161.4	-45.0	156.2
67.1	161.6	-43.6	156.6
69.2	161.6	-42.2	157.0
71.3	161.7	-40.8	157.3
73.4	161.8	-39.3	157.7
75.5	161.8	-37.9	158.0
77.6	161.8	-36.4	158.3
79.6	161.8	-35.0	158.6
81.7	161.7	-33.5	158.8
83.8	161.7	-32.0	159.1
85.8	161.6	-30.6	159.3
87.9	161.5	-29.1	159.6

89.9	161.4	-27.6	159.8
92.0	161.2	-26.1	160.0
94.0	161.1	-24.6	160.2
96.0	160.9	-23.1	160.4
98.1	160.7	-21.6	160.5
100.1	160.4	-20.1	160.7
102.1	160.2	-18.6	160.8
104.1	159.9	-17.1	161.0
106.1	159.6	-15.6	161.1
108.0	159.3	-14.1	161.2
110.0	159.0	-12.5	161.3
112.0	158.7	-11.0	161.4
113.9	158.3	-9.5	161.5
115.9	157.9	-7.9	161.6
117.8	157.5	-6.4	161.7
119.7	157.1	-4.8	161.7
121.6	156.6	-3.3	161.8
123.5	156.2	-1.7	161.8
125.4	155.7	-0.2	161.8
127.3	155.2	1.4	161.8
129.1	154.7	3.0	161.8
131.0	154.2	4.5	161.8
132.8	153.6	6.1	161.8
134.6	153.0	7.6	161.8
136.4	152.4	9.2	161.7
138.2	151.8	10.8	161.7
139.9	151.2	12.4	161.6
141.7	150.5	13.9	161.5
143.4	149.9	15.5	161.4
145.2	149.2	17.1	161.3
146.9	148.5	18.7	161.2
148.6	147.7	20.2	161.0
150.2	147.0	21.8	160.9
151.9	146.2	23.4	160.7
153.5	145.4	25.0	160.5
155.2	144.6	26.6	160.3
156.8	143.8	28.1	160.1
158.4	143.0	29.7	159.8
159.9	142.1	31.3	159.6
161.5	141.2	32.9	159.3
163.0	140.3	34.4	159.0
164.5	139.3	36.0	158.7
166.0	138.4	37.6	158.3
167.5	137.4	39.2	157.9
169.0	136.4	40.7	157.5
170.4	135.4	42.3	157.1

171.8	134.4	43.9	156.7
173.2	133.3	45.4	156.2
174.6	132.2	47.0	155.7
175.9	131.1	48.5	155.2
177.3	130.0	50.1	154.6
178.6	128.8	51.6	154.0
179.9	127.6	53.2	153.4
181.2	126.4	54.7	152.7
182.4	125.2	56.2	152.0
183.7	123.9	57.8	151.3
184.9	122.6	59.3	150.5
186.1	121.3	60.8	149.7
187.2	120.0	62.3	148.8
188.4	118.6	63.8	147.9
189.5	117.3	65.4	147.0
190.6	115.8	66.9	146.0
191.7	114.4	68.3	145.0
192.8	112.9	69.8	143.9
193.8	111.4	71.3	142.8
194.8	109.9	72.8	141.6
195.8	108.3	74.2	140.4
196.8	106.7	75.7	139.1
197.7	105.1	77.1	137.8
198.6	103.5	78.6	136.4
199.5	101.8	80.0	134.9
200.4	100.1	81.4	133.4
201.3	98.3	82.9	131.8
202.1	96.6	84.3	130.2
202.9	94.7	85.7	128.5
203.7	92.9	87.0	126.7
204.5	91.0	88.4	124.9
205.2	89.1	89.8	123.0
206.0	87.1	91.1	121.0
206.7	85.2	92.5	118.9
207.3	83.1	93.8	116.8
208.0	81.1	95.1	114.6
208.6	79.0	96.4	112.3
209.2	76.8	97.7	109.9
209.8	74.6	99.0	107.5
210.4	72.4	100.3	104.9
210.9	70.2	101.5	102.3
211.4	67.9	102.8	99.5
211.9	65.5	104.0	96.7
212.4	63.1	105.2	93.8
212.8	60.7	106.4	90.7
213.2	58.2	107.6	87.6

213.6	55.7	108.8	84.4
214.0	53.1	109.9	81.1
214.4	50.5	111.0	77.6
214.7	47.9	112.2	74.1
215.0	45.2	113.3	70.4
215.3	42.4	114.3	66.6
215.6	39.6	115.4	62.7
215.8	36.8	116.5	58.7
216.0	33.8	117.5	54.6
216.2	30.9	118.5	50.3
216.4	27.9	119.5	45.9
216.6	24.8	120.5	41.4
216.7	21.7	121.4	36.7
216.8	18.5	122.4	31.9
216.9	15.3	123.3	27.0
217.0	12.0	124.2	21.9
217.0	8.7	125.1	16.7
217.0	5.3	125.9	11.3
217.1	1.8	126.7	5.8
217.0	-1.7	127.6	0.1
217.0	-5.3	128.3	-5.7
216.9	-8.9	129.1	-11.7

APPENDIX C

DRIVER ANTERIOR TORSO CONTOURS

All coordinates in mm.

Rifleman Side View Relative to Reference Point

X	Z
210.7	269.7
201.3	262.2
193.1	254.7
187.7	246.2
186.5	245.1
180.1	234.3
171.6	219.9
163.8	209.3
158.7	198.6
157.9	195.5
150.9	184.4
148.4	175.9
143.9	166.2
144.1	164.9
144.2	164.6
143.5	161.1
137.0	149.1
133.0	144.3
121.4	115.3
115.7	106.1
109.7	90.7
107.9	77.6
77.5	22.3
64.6	8.9
58.4	2.2
56.0	-0.4
50.9	-6.8
43.5	-14.8
38.1	-18.5
34.4	-25.3
25.4	-40.6
23.8	-42.2
13.5	-73.3
4.5	-87.0
-3.2	-99.1
-12.7	-121.2
-14.1	-143.1
-14.1	-143.1
-12.7	-165.8
-9.9	-185.8
-2.8	-196.3
5.3	-206.3

Rifleman Top View Relative to Reference Point (Z Value is -121 mm)

X	Y
157.3	401.9
147.2	400.3
128.1	389.4
125.2	386.0
110.4	367.3
100.0	355.8
39.2	291.0
31.8	281.2
17.4	260.7
4.1	239.9
-7.5	222.1
-9.5	212.3
-13.6	178.5
-13.4	177.6
-12.3	30.0
-19.4	5.1
-20.5	-2.2
-20.1	-10.6
-26.1	-33.1
-26.7	-39.1
-30.0	-65.3
-31.4	-72.7
-31.4	-72.7
-18.6	-106.6
-13.1	-120.3
8.5	-138.4
23.3	-143.5
58.9	-165.9
65.9	-169.3
76.0	-174.7
95.9	-187.1
103.5	-194.7
107.6	-197.4
138.3	-220.7
169.1	-239.3
183.4	-244.6

IOTV Side View Relative to Reference Point

X	Z
-138.3	-344.8
-137.9	-344.3
-137.3	-338.9
-135.2	-334.4
-133.8	-329.3
-131.1	-298.7
-132.0	-296.4
-133.3	-292.7
-134.1	-289.6
-134.7	-288.1
-136.1	-284.5
-135.6	-280.4
-135.7	-280.0

-135.3	-276.6
-134.0	-271.7
-133.7	-269.7
-132.6	-267.3
-131.7	-266.1
-130.1	-260.0
-129.8	-259.8
-125.1	-248.0
-124.9	-246.4
-120.0	-239.2
-116.0	-228.0
-115.7	-227.0
-113.5	-214.8
-113.1	-214.8
-108.5	-203.5
-107.5	-201.1
-101.2	-190.1
-97.8	-178.3
-94.5	-168.8
-92.4	-165.7
-91.6	-163.6
-89.7	-157.0
-89.1	-155.8
-87.1	-149.6
-85.0	-146.9
-82.0	-141.3
-81.7	-140.8
-80.1	-139.9
-79.8	-139.2
-54.4	-78.7
-54.7	-75.6
-55.4	-70.1
-54.7	-62.9
-53.5	-58.8
-53.0	-57.7
-52.2	-51.1
-50.2	-44.4
-48.9	-42.1
-47.8	-41.5
-45.3	-40.6
-41.8	-35.1
-38.7	-33.1
-36.1	-30.4
-33.3	-27.4
-31.0	-24.1
-26.8	-18.3
-25.8	-17.9
-19.0	-8.9
-11.8	5.0
-4.7	33.4
-3.7	34.8
-3.0	35.6
-1.2	39.5
3.3	43.3
3.5	43.4
5.3	43.6
12.0	49.3
13.3	49.8

46.4	91.5
47.6	94.1
48.4	95.3
50.1	97.0
53.1	99.1
54.0	99.8
55.1	100.8
57.6	102.4
63.2	107.5
66.1	110.1
68.2	111.9
70.9	114.6
75.6	119.3
80.3	123.4
85.5	127.2
89.2	129.6
94.0	132.0
94.8	132.5
99.5	135.0
101.9	136.7
109.5	139.7
115.1	141.4
118.8	142.0
126.6	143.6
127.3	143.4
149.4	151.8

IOTV Top View Relative to Reference Point

X	Y	Z
58.7	-198.7	-250
48.9	-197.6	-250
48.3	-198.0	-250
45.2	-197.4	-250
36.3	-196.4	-250
34.0	-195.6	-250
28.2	-194.2	-250
27.6	-194.2	-250
22.2	-191.5	-250
16.3	-190.0	-250
15.8	-190.2	-250
12.1	-189.0	-250
10.1	-188.7	-250
1.7	-186.4	-250
-0.6	-185.9	-250
-1.5	-185.3	-250
-4.8	-183.8	-250
-6.1	-183.5	-250
-14.2	-181.8	-250
-18.7	-180.4	-250
-25.5	-178.0	-250
-32.1	-174.8	-250
-34.9	-174.2	-250
-40.3	-171.4	-250
-48.4	-168.0	-250
-51.7	-167.0	-250
-52.8	-166.4	-250

-57.9	-163.8	-250
-63.6	-161.2	-250
-66.9	-159.9	-250
-71.8	-156.7	-250
-75.8	-154.2	-250
-79.5	-153.0	-250
-86.6	-149.2	-250
-88.5	-148.2	-250
-90.7	-147.0	-250
-91.7	-146.1	-250
-92.5	-144.8	-250
-94.1	-141.9	-250
-95.2	-139.0	-250
-95.4	-137.7	-250
-95.7	-134.9	-250
-96.9	-131.4	-250
-96.9	-130.2	-250
-97.3	-123.4	-250
-105.7	-97.8	-250
-109.2	-89.1	-250
-111.7	-79.3	-250
-112.3	-77.2	-250
-113.0	-73.0	-250
-115.4	-63.9	-250
-115.4	-57.5	-250
-116.8	-52.1	-250
-118.2	-46.2	-250
-119.1	-37.8	-250
-120.1	-34.6	-250
-121.3	-25.8	-250
-121.7	-23.2	-250
-123.3	-16.8	-250
-122.9	-11.9	-250
-124.0	-6.5	-250
-124.4	-5.1	-250
-126.6	2.0	-250
-126.6	8.2	-250
-126.9	10.7	-250
-126.4	17.5	-250
-127.3	24.8	-250
-127.0	26.8	-250
-127.0	28.3	-250
-126.7	44.4	-250
-127.2	46.5	-250
-126.8	47.7	-250
-126.3	58.9	-250
-125.1	67.0	-250
-125.1	67.0	-250
-121.9	76.8	-250
-119.7	80.3	-250
-116.7	85.4	-250
-116.6	86.1	-250
-115.2	90.1	-250
-115.1	90.4	-250
-115.1	90.8	-250
-113.5	94.4	-250
-112.3	99.9	-250
-108.7	107.9	-250

-108.4	110.5	-250
-107.0	113.1	-250
-105.4	117.7	-250
-102.6	122.4	-250
-89.4	160.9	-250
-89.0	163.7	-250
-88.8	166.4	-250
-89.3	168.3	-250
-88.2	171.0	-250
-84.7	176.9	-250
-82.8	178.5	-250
-78.9	180.3	-250
-75.8	182.2	-250
-75.3	182.6	-250
-70.4	183.7	-250
-64.2	186.4	-250
-57.8	188.6	-250
-54.9	189.9	-250
-53.8	190.2	-250
-51.1	191.1	-250
-50.2	191.4	-250
-39.6	195.5	-250
-33.7	197.8	-250
-25.3	200.8	-250
-23.6	201.0	-250
-19.1	202.8	-250
-6.5	207.3	-250
0.4	209.0	-250
11.1	211.0	-250
15.5	213.2	-250
24.1	215.7	-250
34.9	218.7	-250
35.2	218.7	-250
38.6	218.8	-250
41.8	219.4	-250